DOI:10.7598/cst2017.1333
ISSN:2278-3458

Chemical Science Transactions
2017, **6(3),** 417-427

RESEARCH ARTICLE

Green Synthesis of Platinum and Gold Nanoparticles and their Self-Assembled Nanostructures

VENU REDDY

School of Engineering Science and Technology, University of Hyderabad, Gachibowli, Hyderabad–500046, India
rvenu8@uohyd.ac.in

Received 25 October 2016 / Accepted 7 November 2016

Abstract: This paper presents a "green" approach for the preparation of platinum (Pt) and gold (Au) nanoparticles and their self-assembled nanostructures by means of *L*-ascorbic acid and sodium carboxymethyl cellulose (CMC) as reducing and stabilizing agents, respectively. The self-assembly structures of Pt and Au nanoparticles such as Pt nanowires, Pt nanodendrites and Au nanochains were achieved by adjusting the experimental parameters. The synthesized metal nanostructures were systematically characterized with transmission electron microscopy (TEM), x-ray diffraction (XRD) and fourier transform infrared spectroscopy (FT–IR) techniques. The selected area electron diffraction, XRD patterns and the high resolution–TEM image confirm that the resulting metal nanostructures are highly crystalline and the structure is face–centered cubic (fcc). The FT–IR analysis suggests that the resulted metal nanostructures are stabilized with –COO– (carboxylate) and –OH (hydroxyl) groups in CMC molecules. It is also noted that the type of interaction between metal particle and carboxylate group is bidentate bridging. The present method provides a simple, cost–effective and eco–friendly strategy toward the fabrication of Pt and Au nanostructures.

Keywords: Platinum, Gold, Nanoparticles, Self-assembly, Green synthesis

Introduction

Now with advances of nanoscience and technology, the use of noble metal nanoparticles such as platinum (Pt) and gold (Au) have been playing an important role in areas of catalysis, nanomedicine and nanoelectronics[1-11]. The procedure is most often used to the chemical synthesis of Pt and Au nanoparticles is the chemical reduction method, which deals with the reduction of Pt/Au precursors to Pt/Au nanoparticles in a solvent medium by means of chemical reducing agents and suitable stabilizing agents. Majority of methods in the literature involves reduction of Pt/Au precursors by toxic reducing agents and/or stabilizing agents and often use of organic solvents, which restrict the scaling-up for industrial applications and are of environmental concern[12–16]. In order to avoid or minimize these restrict conditions, a green synthesis is desirable. As consequences, a number of biological methods have been developed for the synthesis of Pt and Au nanoparticles such as

plant materials (*Moringa oleifera* Lam flower extract, *Commelina nudiflora* L. whole plant, *Sesbania grandiflora* L. Leaf extract, *Punica granatum* L. peel extract, *Sapindus mukorossi* Gaertn. Fruit pericarp *etc.,*) and microorganisms (*Bacillus flexus, Shewanella algae, Inonotus obliquus etc*.,)[17-23,2]. Most of these methods were focused on preparation of nanoparticles not on the self-assembled structures made from nanoparticles. The assemblies of Pt and Au nanoparticles are gained much interest in the field of catalysis. For example, Pt nanowires exhibit a larger catalytic activity than the Pt nanoparticles toward the reduction of *p*-nitrophenol or potassium ferricyanide by sodiumborohydride[24].

To date, two major techniques commonly used for fabricating self-assembled Pt and Au nanostructures. First technique, the template is used to fabricate the self-assembled nanostructures, which is limited by some of restricting factors, for instance, the preparation and removal of the templates required some complex conditions[25-27]. Second technique, metal precursors are reduced by reducing agents in the presence of capping agents or morphology-directing reagents. Only a few methods are reported for the preparation of Pt and Au assembled structures from their nanoparticles. Recently, Chiera and co-workers[28] and Qin *et.al.,*[24] have demonstrated the formation of gold nanowire networks in deep eutectic solvents, such as ethaline or reline and Pt self-organized nanoparticle linked nanowires in NaOH solutions, by reduction of Au ($HAuCl_4$) and Pt (H_2PtCl_6) precursor with sodium borohydride, respectively. Shen *et al*., reported the formation of dendritic structures of Pt, using high cost high-cost instrumental setup such as sonoelectrochemical instrument[29]. These conditions, however, were either use of toxic reducing agents or high-cost instrumental setups; possibly restrict the scaling-up in industrial applications. Thus, there is a great demand to develop efficient synthetic methods that able to prepare the Pt and Au nanoparticle self-ordered assemblies. In this context, the green materials, such as *L*-ascorbic acid (vitamin C), is an inexpensive mild reducing agent[30] and along with the combination of sodium carboxymethyl cellulose (CMC) as the stabilizing/capping agent[31], in an aqueous phase preparation of Pt and Au nanoparticles and their assembled nanostructures would provide "green" conditions and scaling-up properties to this method.

Herein, I report a simple "green" approach for the preparation of Pt and Au nanoparticles and their self-assembled nanostructures, using vitamin C and CMC as reducing and stabilizing agents, respectively. The experimental parameters such as effects of CMC concentration and reaction time periods on the formation of Pt and Au nanostructures were investigated. The type of interaction between metal particle and stabilizing agent were also studied.

Experimental

Hexachloroplatinic acid (H_2PtCl_6), chloroauric acid ($HAuCl_4$), Vitamin C and CMC were purchased from Sigma–Aldrich (USA). The obtained noble metal nanostructures were characterized by means of transmission electron microscope (TEM), x–ray diffraction (XRD) and Fourier transform infrared spectroscopy (FT–IR). TEM, selected area electron diffraction pattern (SAED) and energy dispersive x-ray (EDX) data were obtained on an FEI Technai G2 S–Twin. For TEM analysis, a few drops of the Pt colloidal samples dispersion onto the carbon coated copper TEM grid and dried overnight. XRD measurements were performed on a Bruker's AXS Model D8 Advance powder x-ray diffractometer instrument operated with Cu Kα radiation as the x-ray source (λ= 1.54 Ao). The FT–IR spectra were collected on the Nicolet 5700 thermo scientific instrument with the samples as KBr pellets.

Procedures

Preparation of Pt nanostructures

2 mL of 0.01 M H_2PtCl_6 and 2 mL of 0.01 M vitamin C were added to a beaker containing 96 mL of 0.1 wt% CMC aqueous solution and stirred for 20 minutes taken into two different bottles (each bottle 50 mL) and then the bottles were sealed. The tightly sealed bottles were transferred into a preheated oven kept at 90 ^oC. Each reaction vessel was kept in the oven for two reaction times: 2 and 20 h. In other experiments, the amount of CMC was 0.1 and 0.5 wt% at 2 h reaction time.

Preparation of Au nanostructures

To synthesize Au nanoparticles, 2 mL of 0.01 M $HAuCl_4$ aqueous solution was added to the mixture of 2 mL of 0.01 M vitamin C and 96 mL of 0.1 wt% CMC aqueous solution containing beaker at room temperature. For synthesizing self-assembled Au nanoparticles chain structures, the amount of CMC was 0.5 wt%.

Results and Discussion

The standard reduction potential (SRP) of Au^{3+}/Au^0 (relative to the standard hydrogen potential H^+/H^0 = 0.00V) is 1.498 V. The SRP for $[PtCl_6]^{2-}/[PtCl_4]^{2-}$ is 0.68 V and that for $[PtCl4]^{2-}/Pt^0$ is 0.755 V. The potentials of Au^{3+}/Au^0 is higher than that of $[PtCl_6]^{2-}/[PtCl_4]^{2-}$ or $[PtCl_4]^{2-}/Pt^0$ potentials; the more positive potential species have the greater affinity for electrons and the tendency to be reduced[32]. Therefore, the reduction of Pt(IV) ions requires the heat treatment (approximately 100 ^oC) unlikely to the reduction of Au(III) ions. This is also proved by the experiments performed with and without heat treatments. The sample with heat treatment was shown formation of Pt nanoparticles and the sample without heat treatment was not shown any formation of Pt nanoparticles even after 48 h.

Characterization of Pt nanostructures

Figure 1 displays the TEM images of the Pt colloidal solutions prepared from 0.2 wt% of CMC under the reactions periods of 2 and 20 h. It can be seen that monodispersed, crystalline and spherical shaped Pt nanoparticles (Figure 1a, b). The inset in Figure 1a shows the size distribution histogram of spherical shaped Pt nanoparticles with a narrow size distribution from 3 to 6 nm and an average value of ~5 nm. Interestingly, the longer thermal treated (20 h) sample showed long nanowire networks with average diameters of ~5 nm (Figure 1d, e), which were formed by the self–assembly of spherical shaped Pt nanoparticles with an average diameter of ~5 nm and they continued growing into long nanowire networks. The formation of nanowires networks from nanoparticles can be explained by the following hypothesis. As the reaction time (20 h) of the system increases, the Pt nanoparticles possess higher energy, induced by a larger surface-to-volume ratio and it leads to higher collision frequency which is associated with their greater mobility, the coalescence or attachment of small Pt nanoparticles produced long nanowire networks. The thermodynamic driving force for particle coalescence was achieved by eliminating pairs of surfaces; as a result surface energy could be decreased[33-36].

Figure 1b represents a typical high resolution TEM (HR–TEM) image of the Pt colloidal solution from the 0.2 wt% CMC under the reaction period of 2 h. It displays the oriented and ordered lattice fringes of spherical shaped Pt nanoparticles, the interplanar "*d*" spacing is 0.23 nm, which corresponds to that of {111} plane for fcc structure of Pt. Figure 1e displays the HR– TEM image of Pt colloidal solution from the 0.2 wt% CMC under the reaction period of 20 h. It also shows clear oriented and ordered lattice fringes of Pt nanowire

networks, the "*d*" spacing values of 0.23 and 0.19 nm coincides with that of lattice planes of the Pt fcc structure {111} and {200}, respectively[6,37]. The SAED images of Pt nanoparticles and nanowire networks are shown in Figure 1c and f, respectively. It reflects the five rings {111}, {200}, {220}, {311} and {222} diffraction planes, respectively, which represents the face–centered cubic (fcc) structure of Pt. The XRD spectrum of the Pt nanoparticles and assembled structures (nanowire networks) are shown in Figure 2. Diffraction peaks at two theta = 39.90, 46.47, 67.83, 81.57 and 86.01^{o} correspond to the indexed planes {111}, {200}, {220}, {311} and {222} respectively, which were consistent with the fcc structure of Pt[6]. The obtained Pt nanoparticles are verified to contain the Pt according to EDX studies. The EDX spectrum of Pt–CMC nanoparticles (supplementary Information, Figure S1) confirms the presence of Pt.

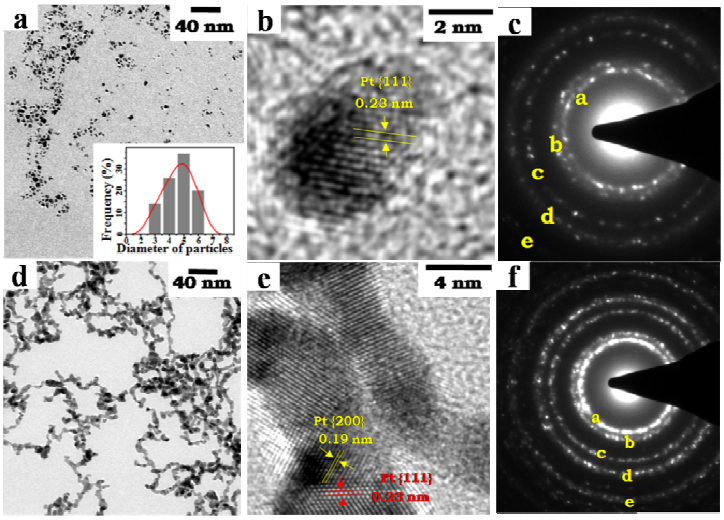

Figure 1. Low resolution and HR-TEM images of the Pt samples reduced in an aqueous solution of 0.2 wt % CMC at different reaction periods: 2 (a,b) and 20 h (e,g). The inset in (**a**) indicates the size distribution histogram of Pt nanoparticles. The SAED patterns of the Pt samples reduced in an aqueous solution of 0.2 wt % CMC under the reaction periods of 2 (**c**) and 20 h (**f**). The five rings denoted "a" to "e" correspond to the {111}, {200}, {220}, {311} and {222} diffraction planes, respectively

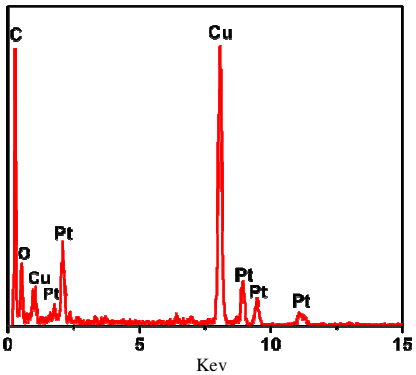

Figure S1. Energy-dispersive x-ray (EDX) spectrum of Pt-CMC nanostrucutres

Effect of CMC amounts on the formation of Pt nanostructures

To investigate the effect of CMC amount on the structural morphology of Pt nanoparticles, I have prepared Pt nanoparticles at low (0.1 wt%) and high (0.5 wt%) amounts of CMC with respect to 0.2 wt% CMC amount. The Pt colloidal sample obtained from a low amount of CMC (0.1 wt%) exhibited heterogeneous structures including spheres, hexagons *etc*., (supplementary Information, Figure S2). Closer inspection of TEM image (supplementary Information, Figure S2) shows spheres (~73%) and hexagons (~24%), along with other shapes (~3%). These heterogeneous structures may be attributed due to the inadequate stabilization of the Pt particles by means of low CMC amount (0.1 wt%).

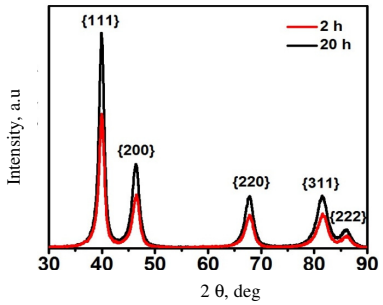

Figure 2. X-Ray diffraction patterns of Pt sample reduced in an aqueous solution of 0.2 wt % CMC at 2 and 20 h reaction periods

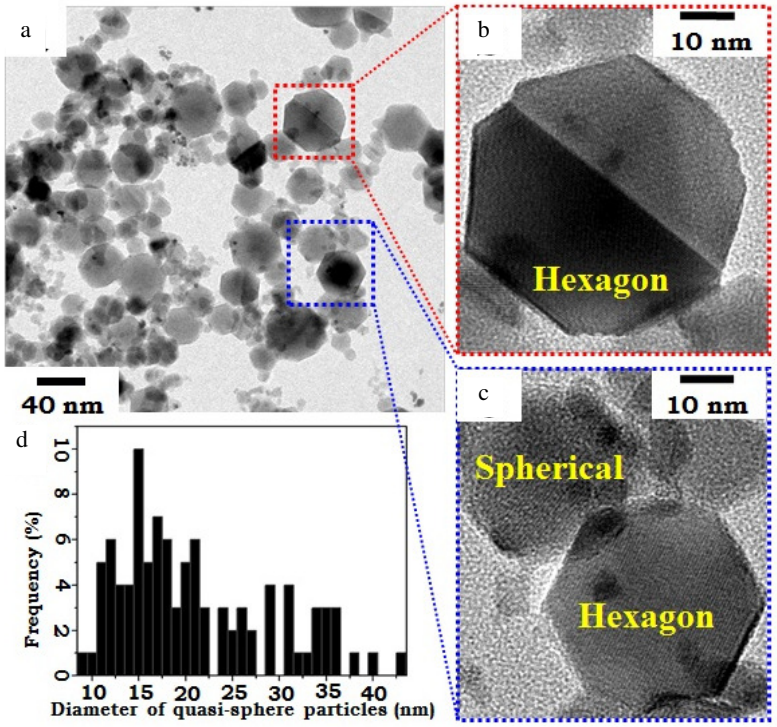

Figure S2. TEM image (**a**), HR-TEM Images (**b-c**) and size distribution histogram (**d**) of the Pt sample reduced in an aqueous solution of 0.1 wt% CMC at 2 h reaction period

The Pt structures obtained from the high amount of CMC (0.5 wt %) under the reaction period of 2 h is shown dispersed spherical dendritic nanostructures (Figure 3a). The size distribution histogram of spherical dendritic structures with a broad size distribution from ~3 to ~16 nm and an average value of ~9 nm (inset in Figure 3a). The dendritic character of the obtained Pt nanostructures is evident in the HR–TEM image (Figure 3b), which is the built upby a few nanoparticles with an average diameter of ~2.5 nm. It appears that these small size spherical nanoparticles are interconnected (assembled) with one another to form spherical dendritic architectures with recognizable boundaries between the component nanoparticles. The HR-TEM image (Figure 3b) shows a lower contrast between the crystallites, which reveals that nanopores separate many small size nanoparticles and also shown the clearly marked interplanar "*d*" spacing value is 0.23 nm. It coincides to that of the {111} lattice planes for fcc metallic Pt (inset in Figure 3b). These dendritic structures are formed due to the use of high amount of CMC (0.5 wt%). Upon use of high amount of CMC, the number of CMC molecules onto the surface of Pt particles is increased with compared to the particles obtained from the use of 0.1% CMC, which leads to the assembly of small size spherical nanoparticles into dendritic structures by the noncovalent interactions between the CMC molecules onto the surface of adjacent Pt particles. Previously, Shen *et al.,* reported that the dendritic structures are prepared by means of high–cost instrumental setup such as sonoelectrochemical instrument[29]. However, in this approach, no high–cost instrumental setups are used to prepare Pt dendritic structures. Therefore, the present green synthetic approach has an advantage to produce Pt dendritic structures in a cost-effective manner.

Figure 3c shows the XRD pattern of Pt colloidal samples were obtained from 0.5 wt% CMC amount at 2 h thermal treatment. Diffraction peaks at two theta = 39.97, 46.39, 67.89, 81.58 and 86.01° correspond to the indexed planes {111}, {200}, {220}, {311} and {222} respectively, which were consistent with the fcc structure of the Pt. These results indicate the CMC amounts can effect only on the structural morphology of the Pt nanoparticle, but not on the crystalline structure of nanoparticles.

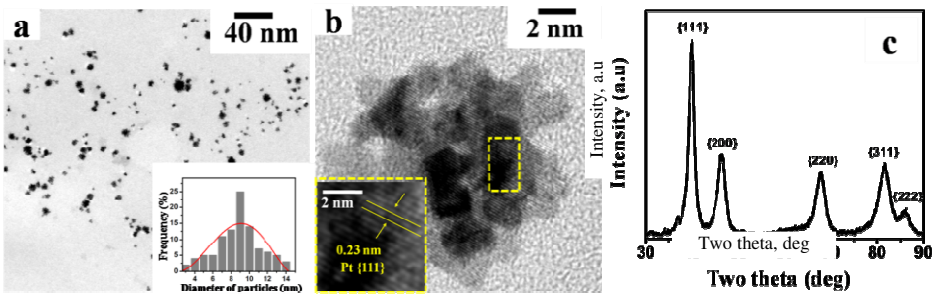

Figure 3. Low resolution TEM image (**a**) and HR–TEM image (**b**) and XRD patterns (**c**) of the Pt sample reduced in an aqueous solution of 0.5 wt % CMC at 2 h reaction period. The insets in (a) and (b) indicates the size distribution histogram of Pt nanodendrites and the clearly marked lattice fringes of dendritic structure, respectively.

Role of vitamin C

The vitamin C contains a free hydroxyl groups, which could be participate in the reduction of metal salts. The reduction of Pt(IV) ions to Pt (0) nanoparticles might be occurring through the oxidation of hydroxyl to carbonyl groups in vitamin C as shown in eq 1:

$$Pt(IV) + 4C_6H_8O_6 \longrightarrow Pt(0) + 4C_6H_7O_6 + 4H^+ \quad (1)$$

Role of CMC

The metal salts (precursors) are reduced by vitamin C in absence of stabilizing/capping agents, the results cloud be in macroscopic pieces of metals that settle out within a few minutes[38]. In order to avoid the formation of macroscopic pieces of metals, a stabilizing agent is needed. Therefore, in this work, a green stabilizing agent is used to attribute metal nanoparticles. Generally, glucose or carboxymethyl cellulose materials have been used as green stabilizing agents for the preparation of metal nanoparticles[15,32]. Among these two, the carboxymethyl cellulose (CMC) is the best choice to stabilize the metal nanoparticles instead of glucose. Because the CMC molecules can make strong interactions with metal surface through bothcarboxylate ($–COO^–$) and hydroxyl (–OH) functional groups, but glucose molecules can make strong interaction with metal surface through only hydroxyl (–OH) groups[15,31].

The FT–IR is used in this work to investigate the interaction between the CMC and Pt nanoparticles. Figure 4a represents the FT–IR spectrum of the neat CMC with no heat processing. The FT–IR spectrum of Pt-CMC nanoparticles (Figure 4b) prepared by means of Vitamin C as reducing agent at 90 ^oC and cooled to room temperature. The previous FT–IR studies have demonstrated that the CMC was not significantly affected by the hydrothermal treatment[15,31]. The FT–IR profiles of CMC (Figure 4a) and Pt-CMC nanoparticles (Figure 4b) revealed that the functional groups in the CMC molecules play an important role in the stabilization of Pt nanoparticles during the synthetic process. The FT–IR spectrum of CMC (Figure 4a) shows the presence of five absorption peaks at 3265, 1588, 1411, 1320 and 1020 cm^{-1}, which are assigned to the stretching vibration of –OH, asymmetric stretching vibration of $–COO^–$, symmetric stretching vibration $–COO^–$, in–plane vibration of –OH and stretching vibration of C–O–C (RCH_2OCH_2R), respectively[31,39]. The FT–IR spectrum of CMC stabilized Pt nanoparticles (Figure 4b) showed some shifts corresponding to stretching vibration of –OH functional group from 3265 to 3420 cm^{-1}, asymmetric stretching vibration of $–COO^–$ from 1588 to 1603 cm^{-1}, symmetric stretching vibration of $–COO^–$ from 1411 to 1418 cm^{-1}, in–plane vibration of –OH from 1320 to 1331 cm^{-1} and stretching vibration of C–O–C from 1020 to 1060 cm^{-1}. These observations suggest that the prepared Pt nanoparticles are stabilized through the interaction of both the $–COO^–$ (carboxylate) and -OH (hydroxyl) functional groups in CMC molecules.

The type of the interaction between a carboxylate group and the surface of Pt particles are identified by the values of wave number separation, Δ, between the asymmetric v_{as} ($–COO^–$) and symmetric v_a ($–COO^–$) stretching vibrations. The Δ value falls in the range of 200-320 cm^{-1} for monodentate (Figure 4c)–one oxygen atom in the carboxylate group covalently bond to the surface of Pt particle, 140-190 cm^{-1} for bidentate bridging (Figure 4c)-Two oxygen atoms in the carboxylate group symmetrically and covalently bond to the surface of Pt particle and <110 cm^{-1} for chelating bidentate (Figure 4c)-Two oxygen atoms in the carboxylate group asymmetrically and covalently bond to the surface of Pt particle[40]. In the present study, the $\Delta(v_{as}\text{-}v_s)$ of 185 cm^{-1} (1603-1418 cm^{-1}) is corresponding to the bidentate bridging interaction.

Characterization of Au nanostructures

The above described method for preparation of Pt nanostructures is applied to prepare the Au nanostructures. The Figure 5 represents the results for Au nanostructures obtained by means of Vitamin C and CMC materials in an aqueous solution at room temperature. TEM image shows the highly monodispersed spherical shaped particles (Figure 5a) produced from 0.1 wt% CMC. The size distribution histogram of spherical particles with a narrow size distribution from ~14 to ~17 nm and an average value of ~15 nm (inset in Figure 5a).

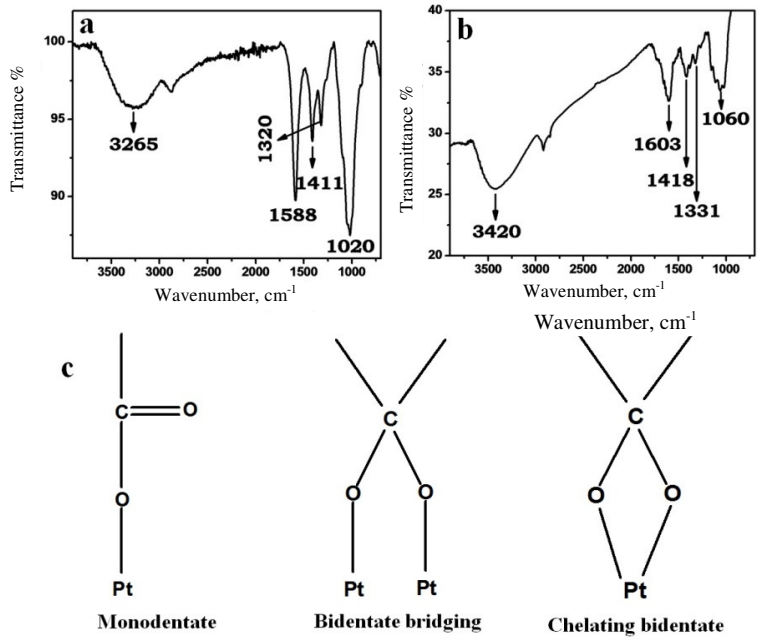

Figure 4. FT–IR spectra of neat CMC (**a**) and CMC stabilized Pt nanoparticles (**b**). Types of interaction between carboxylate group and Pt metal (**c**): monodentate, bidentate bridging, and chelating bidentate

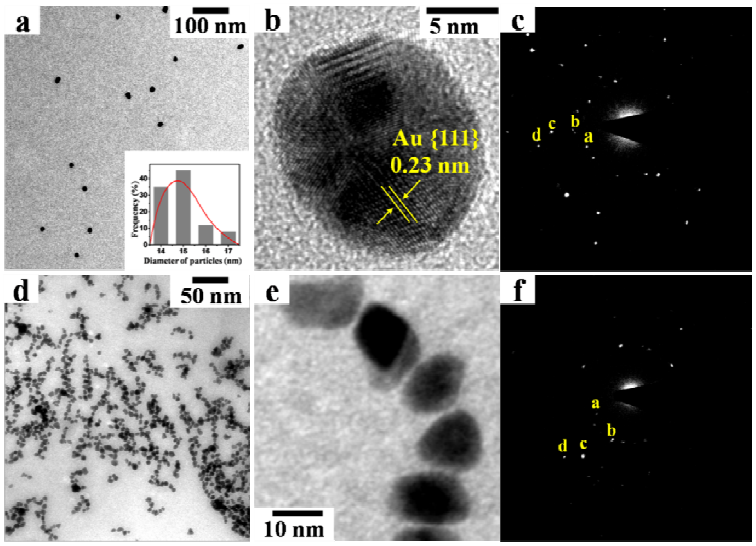

Figure 5. Low resolution TEM image (**a**), HR-TEM image (**b**), the size distribution histogram (**c**) and SAED patterns (**d**) of the Au nanoparticles produced from 0.1 wt% CMC. TEM images (**e-g**) and SAED patterns (**h**) of the nanoparticle chains formed by the self--assembly of Au nanoparticles at 0.5 wt% CMC. The denoted "a" to "d" in SAED images (**d** and **h**) correspond to the {111}, {200}, {220} and {311} diffraction planes, respectively

The characteristic fringes observed from HR-TEM confirm the crystallinity of the as-prepared Au nanoparticles and the interplanar "*d*" spacing is 0.23 nm, which corresponds to that of {111} plane for fcc structure of Au, as shown in Figure 5b. The SAED diffraction patterns were also measured to accesses the crystalline structure of the particles, reflecting the {111}, {200}, {220} and {311} diffraction planes, which represents the fcc structure of Au (Figure 5c). However, the Au nanostructures prepared from the use of 0.5% CMC, the spherical nanoparticles with an average diameter of ~15 nm tend to linear assembling and form chain like structures, which was observed in Figure 5d-f. The SAED patterns in Figure 5f confirm the fcc structure of Au by reflecting {111}, {200}, {220} and {311} diffraction planes. As explained in Pt nanodendrites, similarly, at high amount of CMC (0.5%), the number of CMC molecules anchoring to the surface of Au particles is increased with compared to the particles obtained from the use of 0.1% CMC. Therefore, the discrete Au nanoparticles directed to assembling in the linear way and form nanoparticle chain like structures *via* non-covalent interactions formed between the CMC molecules present on the surface of Au particles.

Conclusion

A simple, cost-effective and eco-friendly synthetic method has been developed for the synthesis of Pt and Au nanoparticles and their self-assembled nanostructures in an aqueous solution at 90 ^{o}C by means of nontoxic vitamin C and CMC as a reducing agent and a capping agent, respectively. The self-assembly of Pt and Au nanoparticles were achieved by adjusting the experimental parameters, such as Pt nanowires were obtained from 0.2 wt% of CMC at 20 h thermal treatment, Pt nanodendrites were obtained from 0.5 wt% of CMC at 2 thermal treatment and Au nanochains were obtained from 0.5 wt% of CMC at room temperature. The resulted metal nanoparticles are stabilized with –COO– (carboxylate) and -OH (hydroxyl) groups in CMC molecules. It is also noted that the type of interaction between metal particle and carboxylate group is bidentate bridging. Thus, the use of CMC as a stabilizing agent and vitamin C as a reducing agent in aqueous phase allowed green chemistry principles to be synthesizing various nanostructures of Pt and Au. This simple green approach can be applied to prepare other metal nanostructures.

Acknowledgement

I would like to gratefully acknowledge the financial support of DST (Department of Science and Technology)–India in the form of INSPIRE Faculty award (IFA13–ENG–70).

References

1. Han G, Ghosh P, De M and Rotello V M, *Nanobiotechnology*, 2007, **3(1)**, 40-45; DOI:10.1007/s12030-007-0005-3
2. Venu R, Ramulu T S, Sunjong O and Kim C G, *Ind Eng Chem Res.*, 2013, **52**, 556-564; DOI:10.1021/ie302037c
3. Daniel M C and Astruc D, *Chem Rev.*, 2004, **104(1)**, 293-346; DOI:10.1021/cr030698+
4. Mashhadizadeh M H and Talemi R P, *Chin Chem Lett.,* 2015, **26(1)**, 160-166; DOI:10.1016/j.cclet.2014.09.004
5. Wang N, Zhao H Y, Ji X P, Li X R and Wang B B, *Chin Chem Lett.*, 2014, **25(5)**, 720-722; DOI:10.1016/j.cclet.2014.01.008
6. Venu R, Ramulu T S, Anandakumar S, Rani V S and Kim C G, *Colloids Surfaces A: Physicochem Eng Aspects*, 2011, **384**, 733-738; DOI:10.1016/j.colsurfa.2011.05.045

7. Polsky R, Gill R, Kaganovsky L and Willner I, *Analy Chem.*, 2006, **78(7)**, 2268-2271; DOI:10.1021/ac0519864
8. Liu S, Zhou X L, Zhang M-M, Lu X, Qin Y J, Zhang P and Guo Z X, *Chin Chem Lett.,* 2016, **27(6)**, 843-846; DOI:10.1016/j.cclet.2016.01.019
9. He YQ, Zhang N N, Liu Y, Gao J P, Yi M C, Gong Q J and Qiu H X, *Chin Chem Lett.*, 2012, **23(1)**, 41-44; DOI:10.1016/j.cclet.2011.10.005
10. Wen Z, Liu J and Li J, *Adv Mater.*, 2008, **20(4)**, 743-747; DOI:10.1002/adma.200701578
11. Li Y, Yang R T, Liu C J and Wang Z, *Ind Eng Chem Res.*, 2007, **46(24)**, 8277-8281; DOI:10.1021/ie0712075
12. Lucia P, Fiorenza R, Paolo S, Fabrizio M and Cesare F N, *Chem Commun.*, 2000, **22**, 2253-2254; DOI:10.1039/B005244M
13. Aika K, Ban L T, Okura I, Namba S and Turkevich J, *J Res Inst Catal Hokkaido Univ.*, 1976, **24**, 54-64.
14. Berceste B, Burcu C and Zehra A, *Gaz Univer J Sci.*, 2009, **22(4)**, 351-357.
15. Juncheng L, Jonathan S and Christopher B R, *J Phys Chem C*, 2007, **111(31)**, 11566-11576; DOI:10.1021/jp071967t
16. Eryza G C, Rodrigo V S, Wido H S, Marcela M O and Aldo J G Z, *Chem Mater.*, 2010, **22(2)**, 360-370; DOI:10.1021/cm902748k
17. Anand K, Gengan R M, Phulukdaree A and Chuturgoon A, *J Ind Engg Chem.*, 2015, **21**, 1105-1111; DOI:10.1016/j.jiec.2014.05.021
18. Palaniselvam K, Mashitah M Y, Solachuddin J A I, Narasimha R P, Gaanty P M and Natanamurugaraj G, *J Ind Engg Chem.*, 2015, **27**, 59-67; DOI:10.1016/j.jiec.2014.11.045
19. Das J and Velusamy P, *J Taiwan Institute Chem Engineers*, 2014, **45(5)**, 2280-2285; DOI:10.1016/j.jtice.2014.04.005
20. Preeti D and Mausumi M, *J Industrial Engg Chem.*, 2015, **22**, 185-191; DOI:10.1016/j.jiec.2014.07.009
21. Muralidharan M, Kevin J P A, Muniyandi J, Navanietha K R and Sangiliyandi G, *J Ind Engg Chem.*, 2014, **20(4)**, 1713-1719; DOI:10.1016/j.jiec.2013.08.021
22. Konishi Y, Ohno K, Saitoh N, Nomura T and Nagamine S, et al, *J Biotechnol.,* 2007, **128(3)**, 648-653; DOI:10.1016/j.jbiotec.2006.11.014
23. Lee K D, Nagajyothi P C, Sreekanth T V M and Soonheum P, *J Ind Engg Chem.*, 2015, **26**, 67-72; DOI:10.1016/j.jiec.2014.11.016
24. Qin G W, Pei W, Ma X, Xu X, Ren Y, Wei Sun and Liang Zuo, *J Phys Chem C*, 2010, **114(15)**, 6909-6913; DOI:10.1021/jp910864w
25. Song Y, Garcia R M, Dorin R M, Wang H, Qiu Y, Eric N Coker, William A Steen, James E Miller and John A Shelnutt, *Nano Lett.*, 2007, **7(12)**, 3650-3655; DOI:10.1021/nl0719123
26. Xue W, Zhao X, Gao D, Gao F, Wang Z, Liyao L and Zhiwei L, *RSC Adv.*, 2015, **5**, 42186-42192; DOI:10.1039/C5RA02921J
27. Zhong L B, Yin J, Zheng Y M, Liu Q, Cheng X X and Luo F H, *Anal Chem.*, 2014, **86(13)**, 6262-6267; DOI:10.1021/ac404224f
28. Chirea M, Freitas A, Vasile B S, Ghitulica C, Pereira C M, Silva F, *Langmuir*, 2011, **27(7)**, 3906-3913; DOI:10.1021/la104092b
29. Shen Q, Jiang L, Zhang H, Min Q, Hou W and Zhu J J, *J Phys Chem C*, 2008, **112(42)**, 16385-16392; DOI:10.1021/jp8060043

30. Murphy C J, Sau T K, Gole A M, Orendorff C J, Gao J X, Linfeng G, Simona E H and Tan L, *Phys Chem B*, 2005, **109(29)**, 13857; DOI:10.1021/jp0516846
31. Juncheng L, Feng H, Tyler M G, Dongye Z, Christopher B R, *Langmuir*, 2009, **25(12)**, 7116-7128; DOI:10.1021/la900228d
32. Yongsoon S, In-Tae B and Gregory J E, *Colloids Surfaces A: Physicochem Eng Aspects*, 2009, **348(1-3)**, 191-195; DOI:10.1016/j.colsurfa.2009.07.013
33. Alivisatos A P, *Science*, 2000, **289(5480)**, 736-737; DOI:10.1126/science.289.5480.736
34. Baneld J F, Welch S A, Zhang H, Ebert T T and Penn R L, *Science*, 2000, **289(5480)**, 751-754; DOI:10.1126/science.289.5480.751
35. Liu X, Stroppa D G, Heggen M, Ermolenko Y, Offenhausser A and Mourzina Y, *J Phys Chem C*, 2015, **119(19)**, 10336-10344; DOI:10.1021/jp5118322
36. Liu X, Koposova E, Offenhausser A, Mourzina Y, *RSC Adv.*, 2015, **5**, 86934-86940; DOI:10.1039/C5RA13931G
37. Yixian W, Xiao Z, Zhimin L, Xiao H, Chaoliang T, Hai L, Bing Z, Bing L, Ying H, Jian Y, Yun Z, Yibin Y and Hua Z, *Nanoscale*, 2014, **6**, 12340-12344; DOI:10.1039/C4NR04115A
38. Victor M S, Nanoscience: Colloidal and Interfacial Aspects, CRS Press, Taylor and Francis Group, Boca Raton, Florida, USA 2010.
39. Nakamoto K, Infrared and Raman Spextra of Inorganic and Coordination Compounds, John Wiley & Sons, New York 1997.
40. Liu J C, He F, Durham E, Zhao D and Roberts C B, *Langmuir*, 2008, **24(1)**, 328-336; DOI:10.1021/la702731h